17th World Conference on Earthquake Engineering, 17WCEE

Sendai, Japan - September 13th to 18th 2020

PERFORMANCE EVALUATION OF SLIDING MODE CONTROL FOR SEMI-ACTIVE SYSTEM ON SEISMIC-ISOLATED STRUCTURE

Y.Mukai[(1)], H. Fujitani[(2)], E. Sato[(3)], E. A. Johnson[(4)], R. Christenson[(5)]

[(1)] *Associate Professor, Graduate School of Engineering, Kobe University, ymukai@port.kobe-u.ac.jp*
[(2)] *Professor, Graduate School of Engineering, Kobe University, fujitani@kobe-u.ac.jp*
[(3)] *Researcher, National Research Institute for Earth Science and Disaster Resilience, eiji@bosai.go.jp*
[(4)] *Professor, Department of Civil and Environmental Engineering, University of Southern California, johnsone@usc.edu*
[(5)] *Professor, Department of Civil and Environmental Engineering, University of Connecticut, rchriste@engr.uconn.edu*

Abstract

In this study, based on the shaking-table test results at the E-defense, the possibility of a semi-active control strategy using a magnetorheological (MR) damper is evaluated in order to improve the seismic-isolation performance of a target base-isolated structure. The test specimen is designed as the single-degree of freedom (SDOF) model. A rigid steel-frame block is supported by the four linear-bearing sliders which are displaceable in a single direction, and the bottom of this block is connected to the base-foundation on the shaking-table by the single natural-rubber-bearing isolator. The natural period of the test specimen is designed initially about 3.9 s, and estimated practically 3.73 s. Single MR damper is installed on the base isolation layer. The MR damper's restoring force is controlled by tuning the applied current on the electrical coil in the range from 0 to 5 A, and the maximum damping force capacity of the MR damper is available up to 10 kN.

The objective of the semi-active control strategy is to give more reduction of the base-isolation layer's deformation while satisfying the condition that seismic-isolation effects, which are indicated by the floor acceleration of the superstructure, is not deteriorated. We focused on a sliding mode control strategy to apply for the semi-active control of the MR damper. For an optimal switching surface in designing the sliding mode control, the index function formed in a linear quadratic regulator (LQR) method is used. The index function contains the response parameters, which are the relative displacement and the relative velocity on the isolation layer. The sensitivity of the weight factor ratio between the displacement and the velocity is estimated through the experimental test. The condition until reaching into the sliding mode is designed to avoid chattering relevant to the phase-changing operation. The whole system design of the controller is considered as that the level of the control forces is applied similarly for every different control test cases.

Experimental test cases are selected for three kinds of parameters of the controller under two kinds of seismic inputs; El Centro (1940) NS by applying scale-factor of 150%, and JR-Takatori (1995) NS by applying scale-factor of 100%. Control performances of these three kinds of parameters of the controller are investigated from the experimental results. Then, each control test case is verified from the comparison between the numerical results and the test results. The reproducibility of the control manipulations is also discussed in this study.

Keywords: Seismic-isolation system; MR damper; Semi-active control; Sliding mode control method

1. Introduction

In 2019, the large-scale test specimen of the seismic-isolation structures was tested using the shaking-table at the E-defense of the National Research Institute for Earth Science and Disaster Resilience (NIED) in Japan. The objective of this project is to examine the possibility of semi-active control to improve the seismic-isolating performance of a target base-isolated structure [1, 2]. The test specimen is designed as the single-degree of freedom (SDOF) model. A rigid steel-frame block is supported by the four linear-bearing sliders which are movable in a single direction, and the bottom of this block is connected to the base-foundation on the shaking-table by the single natural-rubber-bearing isolator. The mass of the steel block is 14900 kg, and the natural period of the test specimen is designed for about 3.73 s. Stiffness of the base isolation system of a natural rubber bearing is evaluated as 42.3 kN/m.

Single magnetorheological (MR) damper is installed at the base-isolation layer, and this MR damper is used for operating the semi-active response control. The MR damper's restoring force can be controlled by tuning the applied current on the electrical coil in the range from 0 to 5 A, and the maximum damping force of the MR damper is available up to 10 kN. The objective of the semi-active control strategy is to give more reduction of the base-isolation layer's deformation while satisfying the condition that seismic-isolation effects, which are indicated by the floor acceleration of the superstructure, is not deteriorated. We focused on a sliding-mode control strategy to apply for the semi-active control of the MR damper. The sensitivity of the control system design parameters to the sliding mode condition is investigated in this study. For this aim, three kinds of control lows having the different gain parameters are selected where the whole system design of the controller is considered as that the level of the control forces is applied similarly for every different control test cases.

Control performances of these three kinds of parameters of the controller are investigated from the experimental results. Experimental test cases have three kinds of parameters of the controller under two kinds of seismic inputs; El Centro (1940) NS by applying scale-factor of 150%, and JR-Takatori (1995) NS by applying scale-factor of 100%. Then, each control test case is verified from the comparison between the numerical results and the test results, and the reproducibility of the control manipulations is investigated.

2. Analytical model and sliding mode control strategy

The test building with the seismic isolation system is regarded as a linear SDOF model; thus, the equation of the motion can be expressed as follows.

$$m\ddot{x} + c\dot{x} + kx = w + u\ . \tag{1}$$

Where *m*, *c*, and *k* are mass (kg), damping coefficient (Ns/m), and stiffness of the isolation layer (N/m), respectively. *x* means the relative displacement (m) of the isolation layer. *u* means the control force (N), which is applied by the MR damper. $w = -m\ddot{x}_0$ is the seismic force input ($\ddot{x}_0$ means a ground acceleration input (m/s^2)). Introducing the state variable $x_1 = x$, $x_2 = \dot{x} = \dot{x}_1$, Eq. (1) can be described in the state space equation form as follow.

$$\dot{\boldsymbol{X}} = \boldsymbol{A}\boldsymbol{X} + \boldsymbol{B}u + \boldsymbol{E}w\ . \tag{2}$$

Where $\boldsymbol{X}$ forms the state vectors as Eqs. (3), and $\boldsymbol{A}$, $\boldsymbol{B}$, and $\boldsymbol{E}$ are delivered as the following matrices in Eqs. (4).

$$\boldsymbol{X} = \{x_1, x_2\}^T, \tag{3}$$

$$\boldsymbol{A} = \begin{bmatrix} A_{11} & A_{12} \\ A_{21} & A_{22} \end{bmatrix} = \begin{bmatrix} 0 & 1 \\ -k/m & -c/m \end{bmatrix},\quad \boldsymbol{B} = \begin{bmatrix} B_1 \\ B_2 \end{bmatrix} = \begin{bmatrix} 0 \\ 1/m \end{bmatrix},\quad \boldsymbol{E} = \begin{bmatrix} 0 \\ 1/m \end{bmatrix}. \tag{4}$$

Here, switching function vector $\sigma(x)$ is introduced as follows [3].

$$\sigma(x) = \boldsymbol{S}\boldsymbol{X} = [S_1 \quad S_2]\boldsymbol{X}\ . \tag{5}$$

When considering the dynamic behavior of the system given by Eq. (2) and Eq. (5), the condition $\dot{\sigma} = 0$ is satisfied while the system state is in the sliding mode. The equivalent control input u_{eq} is determined as follows. Where the seismic force input $\boldsymbol{w} = 0$ is supposed.

$$u_{eq} = -(\boldsymbol{SB})^{-1}\boldsymbol{SAX}\ ,\ \text{where,}\ \det(\boldsymbol{SB}) \neq 0\ . \tag{6}$$

Substituting Eq. (6) into Eq. (2), the equivalent system dynamics under control by the sliding mode can be described as follows.

$$\dot{\boldsymbol{X}} = \{\boldsymbol{I} - \boldsymbol{B}(\boldsymbol{SB})^{-1}\boldsymbol{S}\}\boldsymbol{AX}\ . \tag{6}$$

To determine the optimal switching surface of the sliding mode control, the following index function is introduced in order to minimize the system state variation during the sliding mode state.

$$J = \int_{t_s}^{t} \boldsymbol{X^T Q X} dt\ ,\quad \boldsymbol{Q} = \begin{bmatrix} Q_{11} & Q_{12} \\ Q_{21} & Q_{22} \end{bmatrix},\quad Q_{12} = Q_{21}\ . \tag{8}$$

Where $\boldsymbol{Q}$ is the positive definite matrix. t_s means the time at that the system state has reached to the sliding mode. Eq. (8) can be expressed as follows.

$$J = \int_{t_s}^{t} \{Q_{11}x_1^2 + 2Q_{12}x_1x_2 + Q_{22}x_2^2\} dt\ . \tag{9}$$

By regarding x_2 as the input for the system, Eq. (9) has the LQR form; thus, the optimal solution of the x_2, which can minimize the index function J is given by using the solution P in the following Riccati equation (Eq. (11)).

$$x_2 = -{Q_{22}}^{-1}(A_{12}P + Q_{12})x_1\ . \tag{10}$$

$$2A_{11}P - {Q_{22}}^{-1}(A_{12}P + Q_{12})^2 + Q_{11} = 0\ . \tag{11}$$

Considering Eq. (9) and Eq. (5), the control system can be determined as follows.

$$\boldsymbol{S} = [A_{12}P + Q_{12} \quad Q_{22}]\ . \tag{12}$$

The condition until reaching into the sliding mode is designed by using the following rule.

$$\dot{\sigma} = -G_R\ sgn(\sigma)\ . \tag{13}$$

Where G_R means the reaching mode gain. To avoid chattering behavior due to the switching operation, the saturation function is used instead of the signum function in the Eq. (13).

$$sat(\sigma) = \begin{cases} +1 & when \quad \sigma > L \\ \sigma/_L & when \quad |\sigma| \leq L \\ -1 & when \quad \sigma < -L \end{cases}\ . \tag{14}$$

To determine the control input of the sliding mode controller, the derivative of the system equation given by Eq. (2) and Eq. (5) (when $\boldsymbol{w} = 0$) are operated, then the following expression can be gained.

$$\dot{\sigma} = \boldsymbol{SAX} + \boldsymbol{SB}u\ . \tag{15}$$

Consequently, the control force applied by the sliding mode controller can be given as the following expression by considering Eq. (13) and Eq. (15).

$$u_{SMC} = -(\boldsymbol{SB})^{-1}(\boldsymbol{SAX} + G_R\ sat(\sigma))\ . \tag{16}$$

In this study, a semi-active control using an MR damper is installed on the base isolation system. Thus, the control forces can be applied depending on the direction of the inter-story velocity. Control forces generated by the MR damper is expressed as follows.

$$u_{MR} = \begin{cases} u_{SMC} & when \quad sgn(u_{SMC}) \cdot sgn(\dot{x}) > 0 \\ 0 & when \quad sgn(u_{SMC}) \cdot sgn(\dot{x}) \leq 0 \end{cases}\ . \tag{17}$$

3. Estimation of test results and simulation results

The shaking-table test at the E-defense is performed using the test specimen of the base-isolation model, which has the rigid steel-frame block supported by the linear-bearing sliders. Desplaceable direction of the test specimen is a single direction; thus, this test specimen can be considered as the single-degree of freedom (SDOF) model. The single natural-rubber-bearing isolator is equipped between the steel-frame block and the base-foundation anchoring to the shaking table. Table 1 shows the structural characteristics which are calculated in the initially-designed model and measured on the actually-constructed test specimen.

Table 1 - Specification of the test specimen

Object	Mass (kg)	Stiffness (N/m)	Damping (N s/m)	Natural period (s)
Initial design	14,900	38,500	1437	3.90
Test specimen	14,900	42,300	2000 *	3.73

* Damping coefficient of the test specimen is presumed from the experimental test results.

The objective of this experimental test is to examine the possibility of semi-active control to improve the seismic-isolating performance of a target base-isolated structure. An MR damper is placed on the isolation story of the test specimen. One side of the damper is connected to the steel-frame block, and the other is to the base-foundation on the shaking table. Displacement, velocity, and reaction force of the MR damper are measured in the experiment. When operating a semi-active control on the base-isolation test specimen, the MR damper's restoring force is controlled by adjusting the applied current on the electrical coil in the range from 0 to 5 A. Thus, according to the control lows, the DSP controller manipulates the control current for the MR damper by on-line computation. The maximum damping force of the MR damper is available up to 10 kN. However, the actually-applied current in the experimental test is banned to 4 A.

As described in the previous chapter, our interest is put on the investigation of the control performance using the sliding mode control strategy to apply for the semi-active control of the MR damper. In this study, the sensitivity of the control system design parameters to the sliding mode condition is investigated. For this purpose, three kinds of control cases having the different gain parameters are selected and examined. The whole system parameter design of the controller is considered as that the level of the control forces is applied similarly for every different control test cases. This parameter study was operated before constructing the test specimen. Thus, the structural parameters of the initial model in Table 1 are used to determine controller' gains. The variation of the sliding mode controllers is managed by changing the controller's parameter like the following combination list expression.

$$SMC(i) = \{Q_{11}, Q_{12}, Q_{22,}, G_R\}. \quad (15)$$

In which, Q_{11}, Q_{12} and Q_{22} are the components of the weight matrix of the index function of Eq.(8). G_R is the reaching mode gain to determine the condition until reaching into the sliding mode in Eq.(13). As the parameter to determine the saturation function of Eq.(14), L is fixed to 10 for every controller. Three test cases are explained as follows:

1) $SMC(1) = \{4.675, 0, 1{,}1\}$ **:** The weight-factor for displacement $Q_{11}$is set to larger than the one for velocity Q_{22}.

2) $SMC(2) = \{8.1, 0, 10{,}13\}$ **:** The weight-factor for displacement Q_{11} is set to smaller than the one for velocity Q_{22}; thus, the reduction of the response displacement might be prioritized than *SMC*(1). The reaching mode gain G_R is set to larger than the one of *SMC*(1) to adjust the applied control force level to be nearly equal to *SMC*(1).

3) $SMC(3) = \{93.775, 0, 10, 1\}$ **:** The weight-factor for displacement $Q_{11}$is set to larger than the one for velocity Q_{22} as like *SMC*(1), but the value of both gain Q_{11} and Q_{22} are enlarged. The applied control force level frequently becomes larger than the upper limit of the damper capacity; thus, the clip of the control forces will frequently occur.

El Centro (1940) NS by applying scale-factor of 150%, and JR-Takatori (1995) NS by applying scale-factor of 100% is used in the control test event. Every controller of three kinds is tested under two kinds of seismic inputs.

(1) Control effect comparison

Fig.1, 2, and 3 show the comparison of the experimental results between without control and with control of *SMC*(1), *SMC*(2), and *SMC*(3), respectively. These figures are corresponding to the case of El Centro 150% input. The case mentioned as "without control" is corresponding to the condition that the applied current to the MR damper is always 0 A. By comparing these figures, it is observed that the maximum displacements of the isolation layer can be reduced. The seismic isolation level of floor accelerations of the superstructure is not regarded to be deteriorated. Some spike-like response is observed in the floor accelerations under the controls of *SMC*(1) and *SMC*(2).

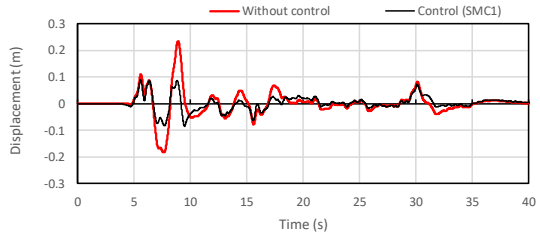

(a) Inter-story displacement (m)

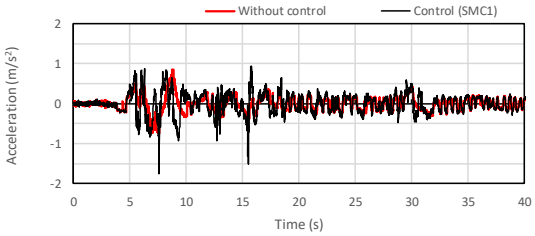

(b) Floor acceleration (m/s^2)

Fig. 1 - Experimental results of of *SMC*(1) and uncontrolled cases (EL Centro NS : 150%)

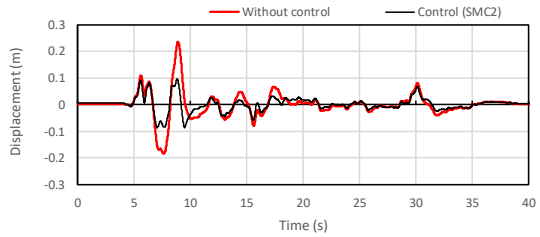

(a) Inter-story displacement (m)

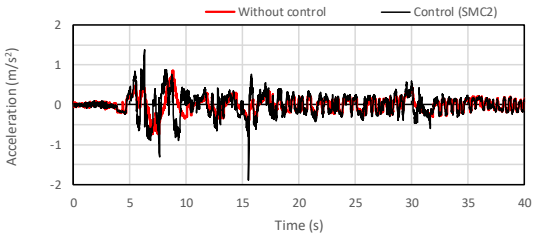

(b) Floor acceleration (m/s^2)

Fig. 2 - Experimental results of of *SMC*(2) and uncontrolled cases (EL Centro NS : 150%)

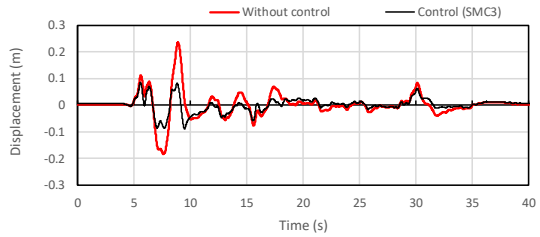

(a) Inter-story displacement (m)

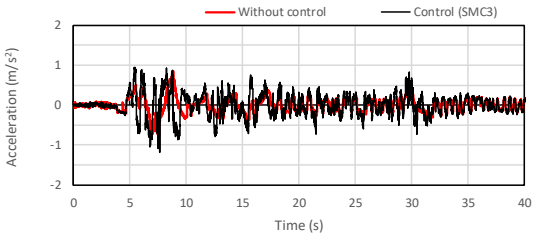

(b) Floor acceleration (m/s^2)

Fig. 3 - Experimental results of of *SMC*(3) and uncontrolled cases (EL Centro NS : 150%)

Fig.4, 5, and 6 show the comparison of the experimental results between without control and with control of *SMC*(1), *SMC*(2), and *SMC*(3), respectively. These figures are corresponding to the case of JR-Takatori 100% input. Unlike the seismic input of El Centro, it is found that the effect of reducing the maximum displacement is not so significant by applying the sliding mode control lows. However, the vibration-convergence performance of the system is thought to be improved by control. The seismic isolation level of floor accelerations of the superstructure is also not regarded to be deteriorated.

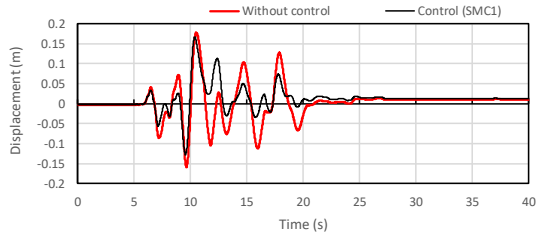

(a) Inter-story displacement (m)

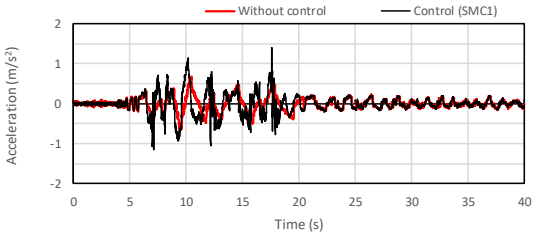

(b) Floor acceleration (m/s^2)

Fig. 4 - Experimental results of of *SMC*(1) and uncontrolled cases (JR-Takatori NS : 100%)

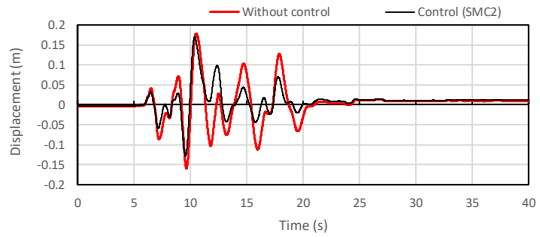

(a) Inter-story displacement (m)

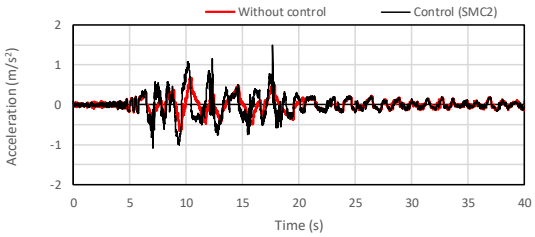

(b) Floor acceleration (m/s^2)

Fig. 5 - Experimental results of of *SMC*(2) and uncontrolled cases (JR-Takatori NS : 100%)

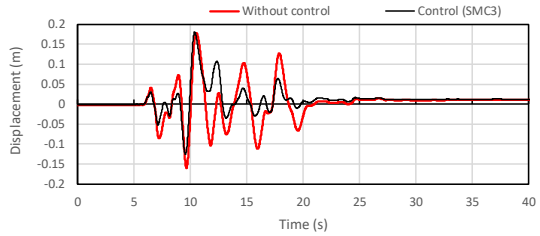

(a) Inter-story displacement (m)

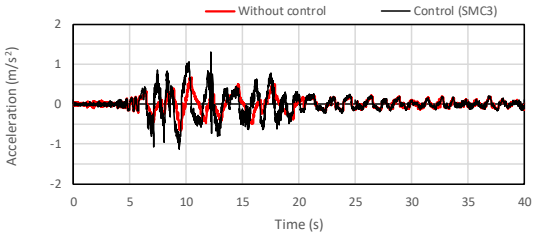

(b) Floor acceleration (m/s^2)

Fig. 6 - Experimental results of of *SMC*(3) and uncontrolled cases (JR-Takatori NS : 100%)

(2) Model parameter calibration of the test structure

In the following, to validate the experimental test results, the numerical simulations are carried out. The structural model parameter survey is carried out to impose the experimental responses in the numerical analysis adequately. As the first step, the structural model parameter survey is carried out on the experimental result of the case without control. Fig. 7 and 8 show a comparison between the experimental results and the numerical simulation results, which are operated on the parameter adjusted model. Fig. 7 and 8 are corresponding to the case of El Centro 150% input and JR-Takatori 100% input, respectively. The numerical model parameter of the model is used from the test specimen's values mentioned in Table 1. Additionally, the non-linear element to express the friction force caused at the linear-bearing sliders is considered in the simulation. The model of the friction force r (N) is expressed as follows.

$$r = -R\, sgn(\dot{x}) \quad . \tag{16}$$

Where *R* corresponds to the maximum static friction force. Through the parameter adjusting process, it is identified to *R* = 1800 (N) in this study. As seen in Fig. 7 and 8, it is observed the numerical simulations can adequately reproduce the experimental test results. In the displacement response, where is depicted on (a) of each figure, there were some margins of errors after the mainshock. However, it is confirmed that the maximum displacements by the simulations can precisely impose on the experimental results.

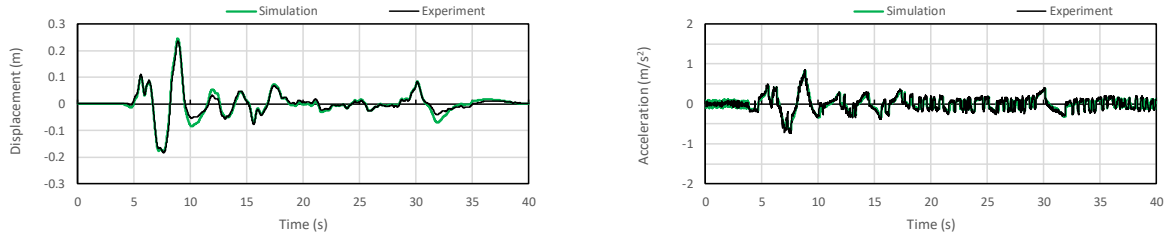

(a) Inter-story displacement (m) (b) Floor acceleration (m/s^2)

Fig. 7 - Comparison of experimental and numerical results of uncontrolled case (El Centro NS : 150%)

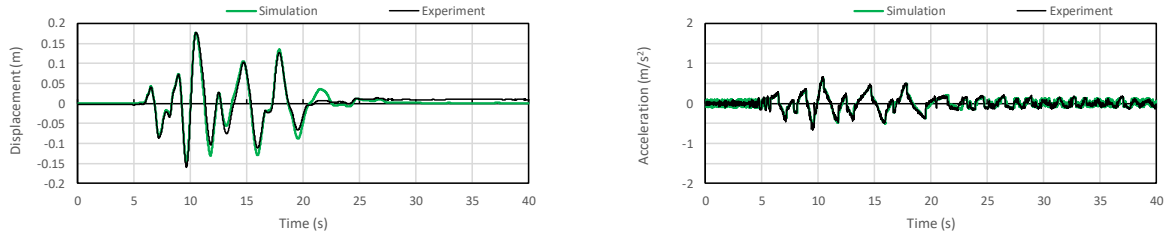

(a) Inter-story displacement (m) (b) Floor acceleration (m/s^2)

Fig. 8 - Comparison of experimental and numerical results of uncontrolled case (JR-Takatori NS : 100%)

(3) Validation of the performance of the sliding mode control

The validation of the experimental test results under the sliding mode control lows, the numerical and the experimental responses are compared. The same numerical model considering the friction forces, which is adjusted for the case without control is used for this aim. Fig. 9, 10, and 11 show comparisons between the experimental results and the numerical simulation results, and these figures are corresponding to the inter-story displacement, the floor acceleration, and the control force applied by MR damper, respectively. In these figures, (a) and (b) correspond to the cases under control of *SMC*(2) and *SMC*(3), respectively. The seismic input motion for these cases is El Centro 150%.

As seen in these figures, the numerical simulation can precisely impose the experimental results. Some spike-like floor acceleration responses which are observed in the experiments do not appear in the numerical results of the control cases (as seen in Fig. 10). In the inter-story displacement, there were some margins of errors partially. As the reason for this, it is considered that the preciseness of the non-linear modeling for the friction forces exists at the linear-bearing sliders. By comparing the control performances between the installation of *SMC*(2) and *SMC*(3), the applied control force using *SMC*(3) is slightly larger than the one of *SMC*(2). The control forces determined by *SMC*(3) is seen to be frequently clipped during the mainshock from 5 s to 10 s in Fig. 11 (b). According to the difference of these control forces, the floor acceleration responses during the mainshock under control of *SMC*(3) became smaller than the case of *SMC*(2). In contrast, comparing the floor acceleration responses after 10 s, the response in *SMC*(3) becomes slightly larger than the case of *SMC*(2), as seen in Fig. 10. About the displacement of the isolation-layer, the response reduction effect is superior in the case of *SMC*(3) across the whole seismic-input duration, because of the higher sensitivity of the control forces applied by *SMC*(3).

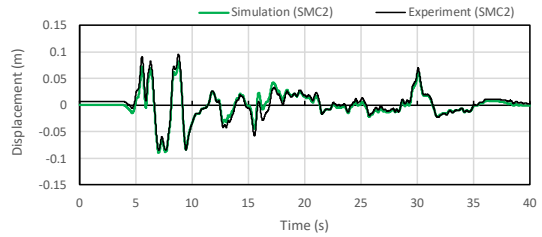

(a) *SMC*(2)

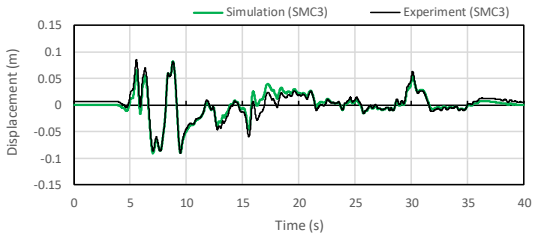

(b) *SMC*(3)

Fig. 9 - Inter-story displacement (m) : comparison of experiment and simulation (El Centro NS : 150%)

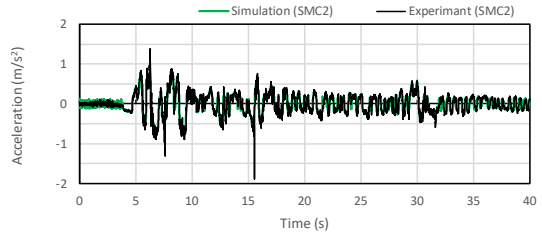

(a) *SMC*(2)

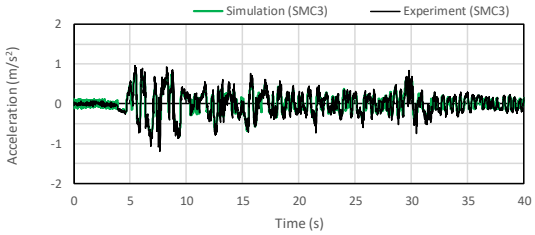

(b) *SMC*(3)

Fig. 10 - Floor acceleration (m/s^2) : comparison of experiment and simulation (El Centro NS : 150%)

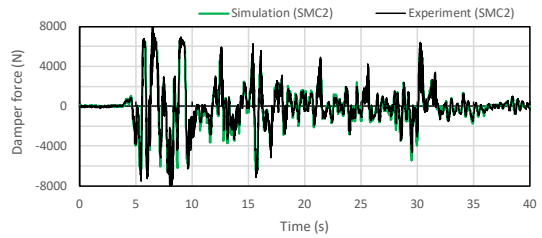

(a) *SMC*(2)

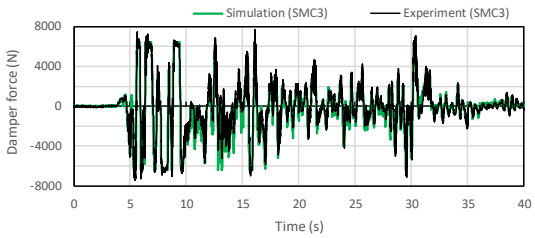

(b) *SMC*(3)

Fig. 11 - Damper force (N) : comparison of experiment and simulation (El Centro NS : 150%)

4. Conclusion

In this paper, the part of the shaking-table test results operated at the E-defense in 2019 is discussed to investigate the possibility of a semi-active control strategy using an MR damper to improve the seismic-isolating performance of a target base-isolated structure. This study focuses on a sliding-mode control strategy to apply for the seismic-isolation building and to evaluate the sensitivity of the control system design parameters to the sliding mode condition. Through the observation of the experimental results, and the comparison between numerical and experimental responses, validation of the experimental results is assured, and the preciseness of the simulations can be confirmed.

Acknowledgments

The part of this study was supported by JSPS KAKENHI Grant Number 18H01587 and JSPS grant No. R2904 in the program for Fostering Globally Talented Researchers.

References

[1] Fujitani H, Mukai Y, Sato E, Johnson E A, Christenson R, Kishida A, Ito M, Shima T, Itahara K, Iba S, Honma A, Fukui H (2020): Comparison of E-Defense Test Results by Five Institutes of Semi-Active Control of Base-Isolation System, *Proc. of the 17th World Conference on Earthquake Engineering (17WCEE)*, Paper No. C001612, 12 pages.

[2] Sato E, Kishida A, Kajiwara K, Fujitani H, Mukai Y, Ito M, Itahara K, Iba S, Johnson E A, Christenson R (2020): Outline of E-Defense Shaking Table Tests for Semi-Active Control of Base-Isolation System, *Proc. of the 17th World Conference on Earthquake Engineering (17WCEE)*, Paper No. C002561, 10 pages.

[3] Nonami K, Tian H (1994): Sliding Mode Control - Theory of non-linear robust control design -, Corona Publishing Co., Tokyo Japan, (in Japanese).

